12

AD

AD-E402 647

Technical Report ARAED-TR-94012

SODIUM "D" EMISSION LINES FROM SELECTED PYROTECHNIC COMPOSITIONS

Patricia L. Farnell

July 1995

US ARMY
TANK AUTOMOTIVE AND
ARMAMENTS COMMAND
ARMAMENT RDE CENTER

U.S. ARMY ARMAMENT RESEARCH, DEVELOPMENT AND ENGINEERING CENTER

Armament Engineering Directorate

Picatinny Arsenal, New Jersey

The views, opinions, and/or findings contained in this report are those of the authors(s) and should not be construed as an official Department of the Army position, policy, or decision, unless so designated by other documentation.

The citation in this report of the names of commercial firms or commercially available products or services does not constitute official endorsement by or approval of the U.S. Government.

Destroy this report when no longer needed by any method that will prevent disclosure of its contents or reconstruction of the document. Do not return to the originator.

REPORT DOCUMENTATION PAGE	Form Approved OMB No. 0704-0188

1. AGENCY USE ONLY (Leave blank)	2. REPORT DATE	3. REPORT TYPE AND DATES COVERED
	July 1995	

4. TITLE AND SUBTITLE
SODIUM "D" EMISSION LINES FROM SELECTED PYROTECHNIC COMPOSITIONS

5. FUNDING NUMBERS

6. AUTHOR(S)

Patricia L.Farnell

7. PERFORMING ORGANIZATION NAME(S) AND ADDRESSES(S)
ARDEC, AED
Energetics and Warheads, Division
(AMSTA-AR-AEE-P)
Picatinny Arsenal, NJ 07806-5000

8. PERFORMING ORGANIZATION

9.SPONSORING/MONITORING AGENCY NAME(S) AND ADDRESS(S)

ARDEC, DOIM
Information Research Center (AMSTA-AR-IMC)
Picatinny Arsenal, NJ 07806-5000

10. SPONSORING/MONITORING AGENCY REPORT NUMBER

Technical Report
ARAED-TR-94012

11. SUPPLEMENTARY NOTES

2a. DISTRIBUTION/AVAILABILITY STATEMENT
Approved for public release; distribution is unlimited.

12b. DISTRIBUTION CODE

13. ABSTRACT (Maximum 200 words)

The broadening of the sodium (Na) D-line emission was studied in detail. It was found that higher flame temperature causes more broadening, and that there is an interaction between Na and nitrogen (present either in an oxidant or an additive) which enlarges an emission shoulder 550 nm and greatly increases the broadening D-lines. Calulations of the energy output of the visible spectra were made and compared to the theoretical black body energy. In addition, calulations were made of the energy possible if each sodium atom emitted one photon.

14.SUBJECT TERMS
Sodium Line broadening
D lines Visible emission
Spectra

15. NUMBER OF Pages
38

16. Price Code

17. SECURITY CLASSIFICATION OF REPORT	18. SECURITY CLASSIFICATION OF THIS PAGE	19. SECURITY CLASSIFICATION OF ABSTRACT	20. LIMITATION OF ABSTRACT
UNCLASSIFIED	UNCLASSIFIED	UNCLASSIFIED	SAR

NSN 7540-01 280-5500
89)
Prescribed by ANSI Std. Z39-18
298-102

Standard Form 298 (Rev. 2-

CONTENTS

FIGURES

TABLES

INTRODUCTION

When sodium nitrate ($NaNO_3$) was first used in illuminating flares, an increase in the visible radiation was achieved. The color of the flame was yellow, instead of white as it had been in the old flares, but this did not constitute a problem. The interesting occurrence was the cause of the radiation; it consisted largely of a very broad spectral line at the wavelength for sodium emission superimposed on a relatively low intensity grey body continuum. This radiation has been extensively studied (ref 1 and 2), and theoretical and experimental studies (refs 3 through 5) have been done to increase the radiation, but a thorough understanding has not been achieved of the process causing this broadened emission. B. E. Douda, however, has proposed a radiative transfer mechanism which works well for magnesium-sodium nitrate flame (refs 5 and 6).

The current study reported here observes the spectral emission obtained from compositions in which the fuel and oxidant types were changed, and the effect of casting and of additives on this emission.

EXPERIMENTAL PROCEDURES

Compositions used in these experiments were consolidated in 2.54 cm diameter Kraft paper cases. A plug of fireclay was placed on the bottom of the composition and an igniter composition was placed on the top. The loading pressure used was 10,000 PSI for the pressed compositions, while two compositions were cast by pouring the composition into the case and hand tamping it.

The flares were burned in the hearth of a standard flare tunnel. Ignition was achieved by burning a piece of ignitacord placed in contact with the igniter composition; the resultant light output was measured by an EG&G radiometer with an ICI corrected response, the output of which was recorded on an oscillographic recorder as candles (c) verses seconds (s). The light was also observed by a Warner-Swasey fast scan optical spectrometer which recorded the spectra as watts (W) versus nanometers (nm), with a resolution of 1 nm. Photographic records of the flames were made with a motion picture camera, and flame shape and dimensions were determined from the films.

The reported parameters are burning time (BT) in seconds, burning rate (BR) in cm/s, luminous output (LO) in c/cm^2 of burning surface and luminous efficiency (LE) in c-s/g of composition. Spectral energies are in watts, as are the calculated thermodynamic quantities.

The appendix lists the equations used to calculate the various other parameters in the tables. The basic equation is the Planck Black Body (BB) equation (app, eq 1), in which the intensity for a particular wavelength and temperature is calculated.

In table 1, the flame temperatures were obtained by calculating the ratio of intensity from the Planck equation 1(app) for a temperature at two different wave lengths, comparing with the ratio of the grey body background at those wavelengths, and trying new temperatures until the ratios agreed within 0.001%. The emissivity of the peak was calculated from equation 2 (app) and of the grey body from equation 3 (app), and the peak/total energy from equation 5 (app).

In table 2, the spectral energies were found by integrating the area under the intensity-wavelength curve and the specific energy was obtained by dividing the spectral energy by the flame area. The percent BB in the 450 to750 nm range was obtained by doing numerical integration of the Planck equation in the range and dividing it by the energy calculated from the Stefan-Boltzmann equation. The expected BB energy was calculated from equation 4 (app).

Table 3 uses equations 6 and 9 (app) to calculate the heat, with the available energy being the difference between them. The percent of spectral/available energy is determined by equation 10 (app), and lists the fraction of energy actually produced from the spectral radiation.

Table 4 uses equation 12 (app) to calculate the possible emission energy from Na. The actual energy in the peak is calculated by multiplying the spectral energy by the percent of peak to spectral energy in tables 1 and 2.

RESULTS

The compositions which were employed in these studies are listed in table 5. Composition 1513 was the basic Mg-Na NO_3 composition; No. 1511 contained Na only as an impurity, mostly in the ammonium nitrate (NH NO_3) while for No. 1512, only 5% of the oxidant was $NaNO_3$. Number 1514 demonstrated the effect of using a different oxidant anion (ClO_3), whereas 1516 and 1517 used different fuels. Numbers 1518 and 1519 illustrated the effect of casting and of the nitrogen-containing additive triethylene glycol dinitrate (TEGDN), and finally, 1515 used a different alkali metal (Li) in the oxidant.

Table 6 presents the burning output data from these compositions. Numbers 1511 and 1512, which contain mostly the nonemitting oxidant NH_4 NO_3, were very slow burning with very low LO and LE, but replacement of only 5% of the NH_4 NO_3 with ($NaNO_3$) resulted in the doubling of LO and LE. Number 1514 produced lower

LO and LE values than did 1513, partly because the sodium anion ($NaClO_3$) contains less Na on a weight percent basis. The apparent intensity from 1515, which contains Li rather than Na in the oxidant, would be greatly reduced by the ICI correction since the emission from Li is mainly in the red region where the sensitivity is quite low. The substitution of aluminium (Al) or carbon (C) as fuel reduced the output, as can be seen by comparing the outputs from 1516 and 1517 with 1513. Casting the composition rather than pressing it caused a reduction in LO and LE; however, the amount of $NaNO_3$ had to be reduced by about 40% to allow for the large amount of binder needed for the cast composition; the addition of TEGDN caused a large increase in BR and produced an LE almost as large as for the pressed composition, with a larger LO due to the high BR. Let us now turn to an analysis of the spectra of the burning compositions. Figures 2 to10 are plots of the efficiency spectra in the region of the alkali metal resonance D lines, as obtained by the Warner-Swasey spectrometer (efficiency spectra were used to eliminate the large changes in intensity caused by changes in the BR); the broadening of the Na and Li lines (superimposed on the grey body continuum caused by incandescent fuel particles) can clearly be seen in all of the spectra from compositions in which the alkali metal oxidant was present as a major constituent; indeed, the emission produced over the region of 450 to 750 nm was largely due to the broadened lines. One interesting feature is the shoulder occurring at 550 nm on the broadened Na line; this shoulder did not appear when carbon was used as a fuel, nor could a shoulder be observed on the broadened Li line; while it did occur when using the $NaClO_3$ oxidant, it was very small for this composition. It thus appears that the shoulder is caused by an interaction between Mg (or Al), Na, and nitrogen, the latter mainly from the oxidant or an additive such as TEGDN.

Table 7 lists the peak widths at half heights for the D-lines on these spectra, while figures 11 to 18 depict more clearly the effect of altering the composition on the shape and size of the Na line. In figure 11, we can see that the addition of only 2.5% $NaNO_3$ caused a doubling of the peak height and the beginning of the broadening effect from the increased concentration of Na as compared with an impurity only. In figure 12, the full broadening effect caused by using $NaNO_3$ can be observed, while the impurity peak from the composition using NH_4NO_3 is almost lost in comparison. It is interesting to note that the grey body continuum was considerably higher for number 1513, as is evident from the data in table 1; part of the increase could be attributed to a higher temperature flame which produced more grey body emission, but a large increase in the grey body emissivity had also taken place.

Figures 13 and 14 illustrate the effect of casting the composition instead of pressing it. In figure 13, the cast composition (1518) was seen to generate very narrow lines compared with the pressed one (1513); however, the addition of TEGDN to the cast composition (1519) produced a higher spectral efficiency and broadening comparable to that from 1513 (fig.14). Figure 15 clearly shows the effect of TEGDN on the cast composition.

If a fuel other than Mg was used, the spectral efficiency was greatly reduced, as can be noted in figure 16. Number 1516, which contained carbon, produced a tiny peak while No. 1517, which contained Al, had the broadest Na lines but generated a much lower spectral efficiency than that of the Mg composition (no. 1513).

Use of the non-nitrated oxidant $NaClO_3$ gave relatively narrow lines compared with those from $NaNO_3$ as illustrated in figure 17. This fact suggests that the broadening was enhanced by the interaction of Na with the nitrate of the oxidant. This observation was corroborated by the effect of adding TEGDN, a nitrated compound, as discussed previously. This interaction will occur for any alkali metal, as demonstrated in figure 18 by the use of $LiNO_3$ instead of $NaNO_3$; however, the Na lines were much broader than the Li ones, indicating a stronger interaction for Na.

Figure 1 depicts the flame shape and size obtained from the motion picture films of the flames from the burning compositions. The flame areas were the cross-sectional areas which were also observed by the Warner-Swasey spectrometer. Analyses of the spectra, combined with the flame sizes, yield the data listed in table 2, while table 3 presents the thermodynamic data and compares it with the spectral outputs.

DISCUSSION

One unexpected result obtained from the data in table1 is that the fraction of total emission which is contained in the Na (or Li) peak was about the same for all the compositions except for number 1511 in which Na was present only as an impurity. This was a rather startling occurrence, since the output of the compositions ranged from 20 to 10,000 Ws. For numbers 1512, 1518, and 1519, which produced similar flame temperatures, the Na line width ranged from 4 to 138 nm, but there was a concomitant increase in the grey body emissivity to maintain the same fraction of radiation in the two parts of the spectra. This change in emissivity yielded an amount of grey body emission which was not solely dependent on the flame temperature and size. On the other hand, peak widths ranged from 4 to 80 nm for compositions with the same grey body emissivity, yet the same fraction of spectral energy was preserved. This latter result was caused by the production of lower spectral peaks which compensate for wider lines. These developments indicate that the increased emission from Na containing compositions is not a simple phenomenon involving only the Na, but a complex interaction with the fuel as well.

The effect of nitrate on the Na emission can easily be seen by comparing number 1513 with number 1514 and number 1518 with number 1519. In the first case, the Na lines were considerably narrower for the composition containing the chlorate oxidant rather than the nitrate one; in the second case, the lines were much broader for the composition containing TEGDN. This latter instance is rather interesting since the

temperature and the amount of Mg and $NaNO_3$ was the same for both compositions, the only difference being that half of the binder was replaced with TEGDN for number 1519. Yet this composition generated lines that were three times broader than number 1518; in fact, the lines were as broad as those for number 1513, even though there is only half as much $NaNO_3$ in number 1519. An argument might be made that the much faster burning of number 1519 would produce greater pressure (although the tenfold increase in flame size should alleviate this situation), but this would definitely not be the case when considering numbers 1513 and 1514; here the faster burning composition has the narrower line.

Now compare the spectral energy that is possible. In table 2, it is seen that for the compositions in which NH_4NO_3 was the primary oxidant, the spectral energy actually achieved was only about 1 1/2% of the possible BB energy; however, the use of a Na containing oxidant increased this percentage by a factor of three or more. Even the extremely low intensity of the composition containing carbon as a fuel achieved 6% of the possible energy (a percentage equivalent to the composition with Mg as fuel); this achievement was possible since the low flame temperature would produce a low theoretical BB energy, partially offsetting the very low intensity produced by the flame. The composition containing TEGDN realized another three to fourfold increase to nearly 20% of the possible energy; this further increase reflects both the higher grey body emissivity and the broad and intense Na peak.

An examination of the thermodynamic data in table 3 shows that the visible radiation emitted by the burning compositions did not account for a large amount of the available energy (that is, the energy from the reaction that is not used to heat the reactants), so that there would be a lot of emission in spectral regions other than the visible. For a grey body emitter, the percent of spectral energy to total energy should be the same as the percent energy for a BB calculated in this region to the total energy. For number 1516, the radiation was less than 1/2% of that available, considerably less than the percentage of BB energy, but numbers 1513, 1514, 1515, and 1519 yielded percentages greater than that for the BB, so that the visible radiation energy produced by these compositions, while low when compared with the total energy, was higher than would be expected. This indicates that the grey body emissivity of these flares could never approach one since the energy would then be greater than the total energy available from the reaction. Of course, this can not happen, so it would suggest that there must be regions of low emissivity outside the 450 to 750 nm region. Measurements of the infrared mission of these compositions confirmed this suggestion, since they did show a low grey body continuum with only a single peak from carbon dioxide emission (ref 8).

Let's now engage in an exercise in conjecture. Table 4 presents the emission energy which would be expected if each atom of Na (or Li) emitted one D-line photon, and if all emitted photons were observed and measured.

Since many of the photons would be absorbed before exiting from the relatively opaque flame, we would expect to calculate a much higher energy than was actually present in the Na peak, reflected in a percentage of calculated-to-observed energy greater than 100%. This did certainly occur for number 1516, in which, evidently because of the low flame temperature, most of the Na emission was absorbed internally. It is indicated that such a mechanism was also operating in the flames for numbers 1517 and 1518; however, for numbers 1514 and 1515, the possible energy is only double the peak energy, a borderline situation at best. For numbers 1512, 1513, and especially 1519, the line is crossed into impossibility; it is not possible to produce the observed Na peak by having each atom emit only once, when one allows for some absorption of the emission by other species in the flame. It thus appears that an entirely different radiation mechanism is operating for these three compositions.

CONCLUSIONS

The available radiation produced by the burning reaction between a fuel and an inorganic oxidant is primarily due to the grey body continuum from hot incandescent particles and to spectral emission from atoms in the oxidant. There is usually a peak from Na D-line emission, even when Na is present only as an impurity. The addition of a small amount of a Na containing oxidant or additive broadens this peak somewhat, but the use of an oxidant containing Na as a cation causes a large amount of broadening. This broadening produces a peak which provides half of the total energy in the spectrum.

It appears that the temperature of the flame has an effect on the magnitude of this broadening. In a cast composition in which there is a large amount of an organic binder, the flame temperature is somewhat lower and the lines are much narrower than for a pressed composition. The use of carbon as a fuel yields the same results, i.e., a cooler flame and narrow lines.

There is an interaction between Na and nitrogen (present either in the oxidant or an additive). This interaction enlarges an emission shoulder which appears at 550 nm, but more importantly, it greatly increases the broadening of the Na D-lines; thus the lines for a composition containing $NaNO_3$ are broader than for one containing $NaC10_3$ while the addition of TEGDN triples line width for a cast composition to the equivalent of a pressed one. The fuel, however, is not passive in this phenomenon; the use of carbon as a fuel generates very narrow lines while Al produces broader lines than does Mg, although the intensity of the peak is much lower for the Al composition. While the lower temperature would perhaps account for the narrow lines for the carbon fuel composition, a temperature effect could not be the cause of the very broad lines for Al fuel, since this composition reaches a lower temperature than does the Mg one. Likewise, the temperature effect, if any, is inoperative for the composition containing TEGDN, since it reaches the same temperature as does the cast composition discussed in the previous paragraph.

The fuel is primarily responsible for the grey body continuum, since it produces hot incandescent particles in the combustion process, yet even in this process, there is an interaction; changing the $NaNO_3$ content from a small fraction of the oxidant to the sole oxidant causes a threefold increase in the emissivity of the grey body continuum. The emissivity is relatively unaffected as the type of fuel, type of oxidant, or type of alkali metal in the oxidant is changed; even casting the composition does not change it; however, addition of TEGDN causes another threefold increase in the emissivity. In fact, except for the composition in which Na is only an impurity, the grey body emissivity (and hence the energy) increases as the energy in the peak increases. Clearly, these changes would have an important effect on the total energy output of the burning composition.

The energy output of the visible spectra of these compositions is only one third, at most, of the available energy from the reaction; however, for several of these compositions, this fraction is greater than the fraction of the black body energy that would fall in this region. Since the infrared energy is very low compared with a black body, no physical laws appear to be broken, but this again points out the inordinate amount of energy which is produced by the Na lines.

This large amount of energy is indeed caused by processes other than the simple thermal excitation and subsequent emission of the D-line photons. For several of the compositions, the energy contained in the peak is greater than could be produced if each atom emitted one photon. This implies a mechanism for excitation other than the thermal process, and one which would have to alter the wavelengths enough to produce the broadened peaks. A radiative transfer model has been developed by Douda (ref 5 and 6), but it must be able to fit all the phenomena described herein to be correct. Since it does not address the grey body continuum emissivity at all, it appears that some more work may be required.

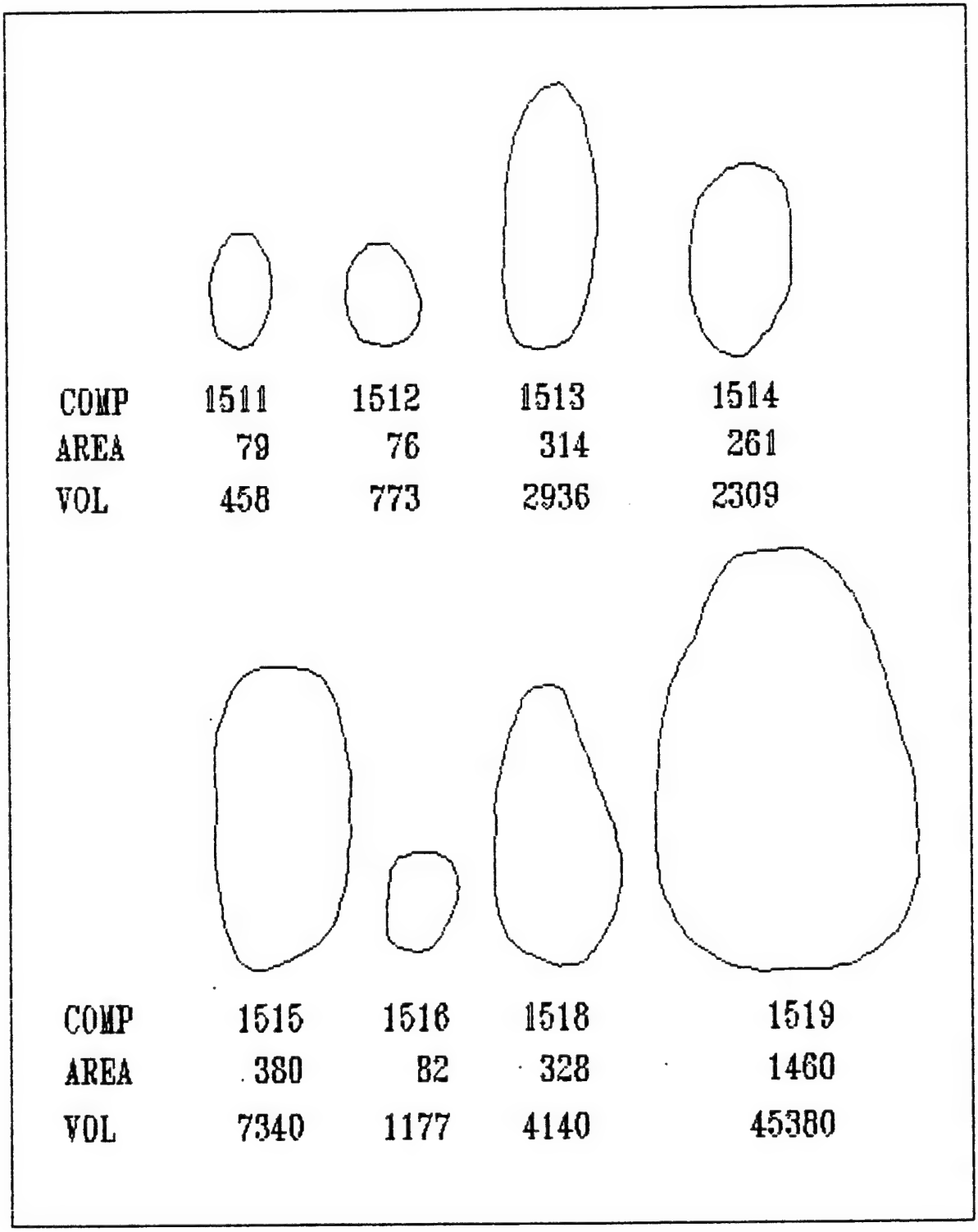

Figure 1
Flame shapes, cross-sectional areas, and volumes (assuming cylindrical symmetry)

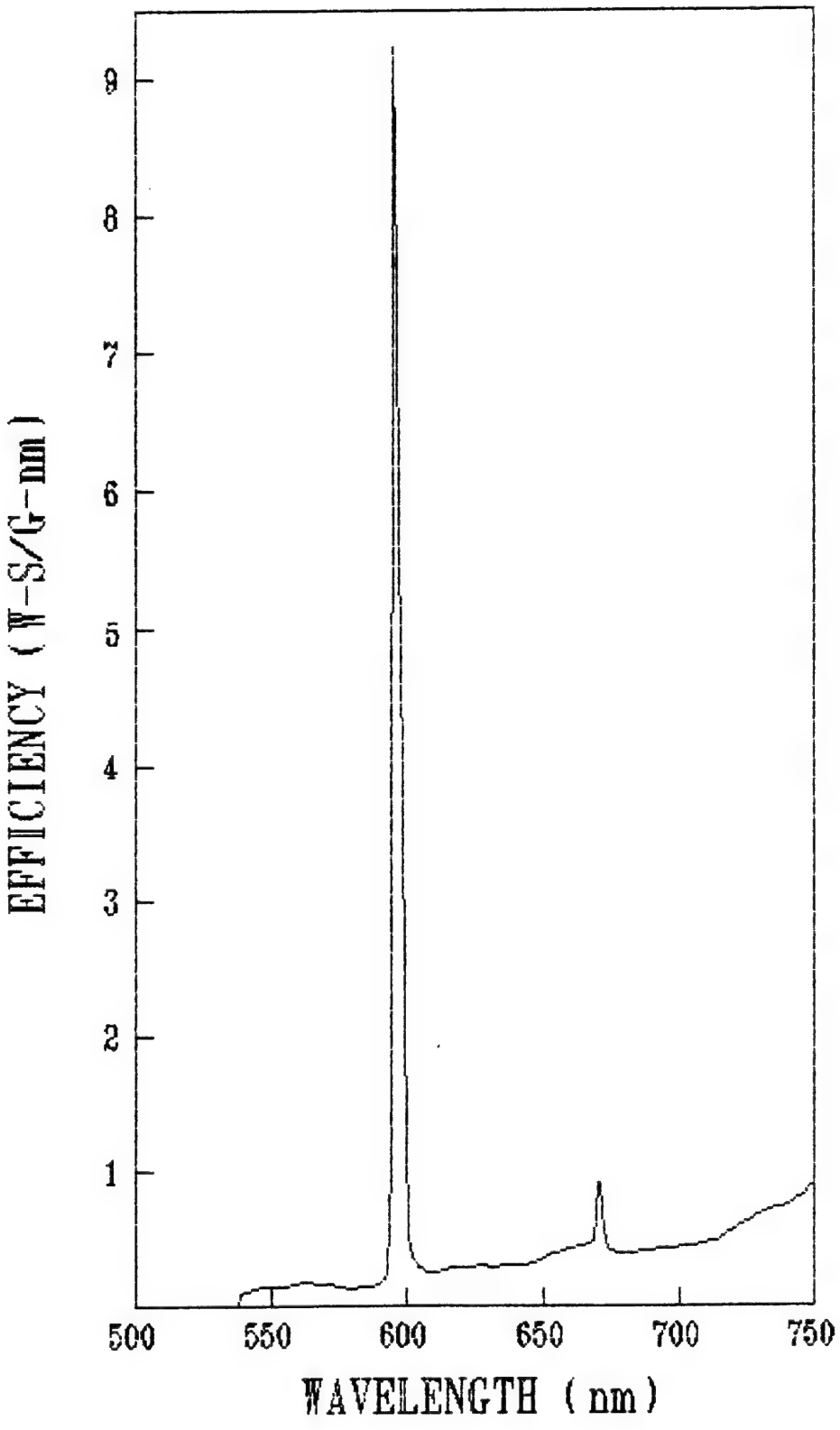

Figure 2
Spectrum of Mg-NH_4NO_3 composition showing Na impurity emission line

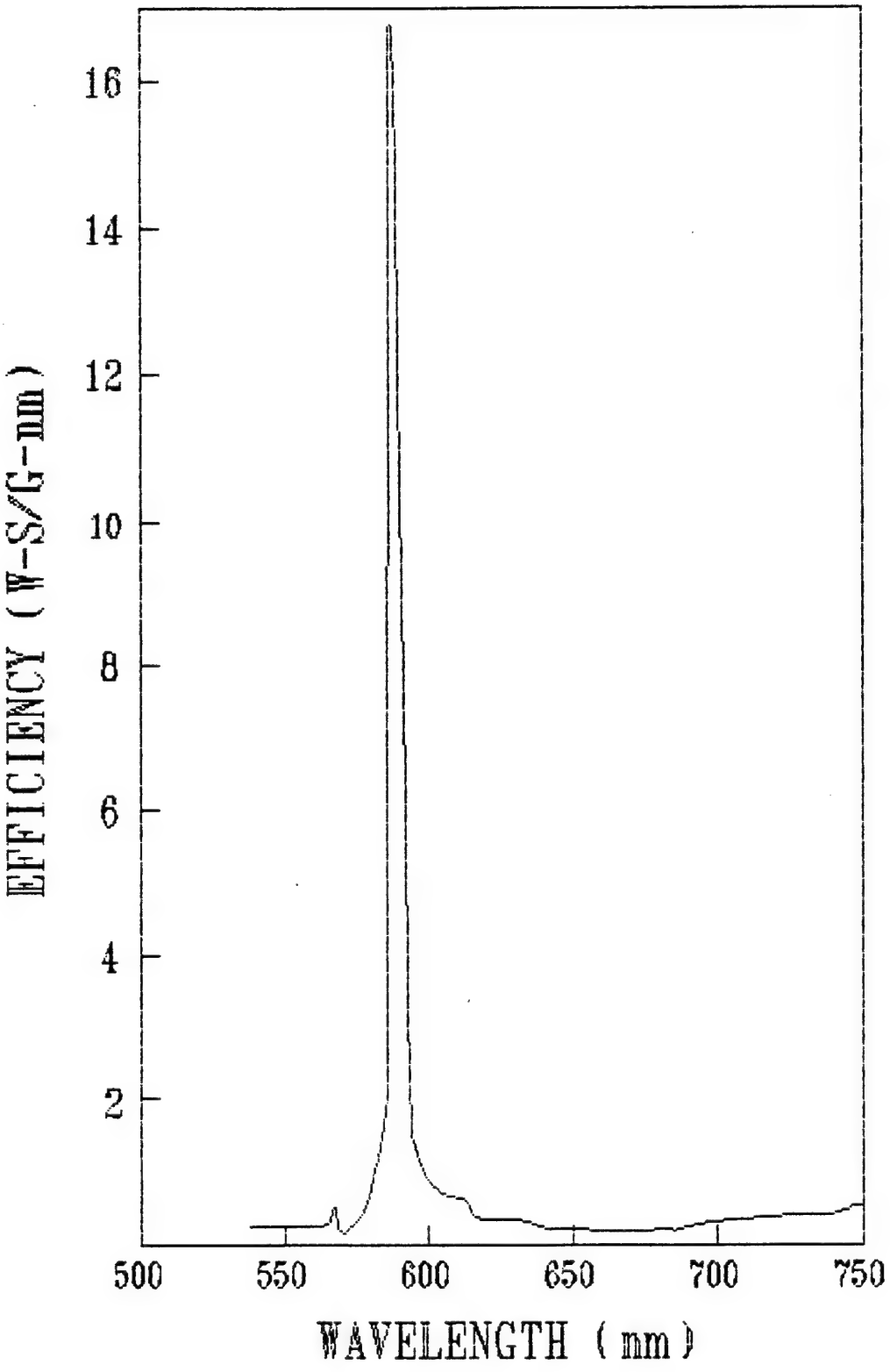

Figure 3.
Spectrum of Mg-NH_4NO_3 composition showing Na emission line from a small amount of $NaNO_3$

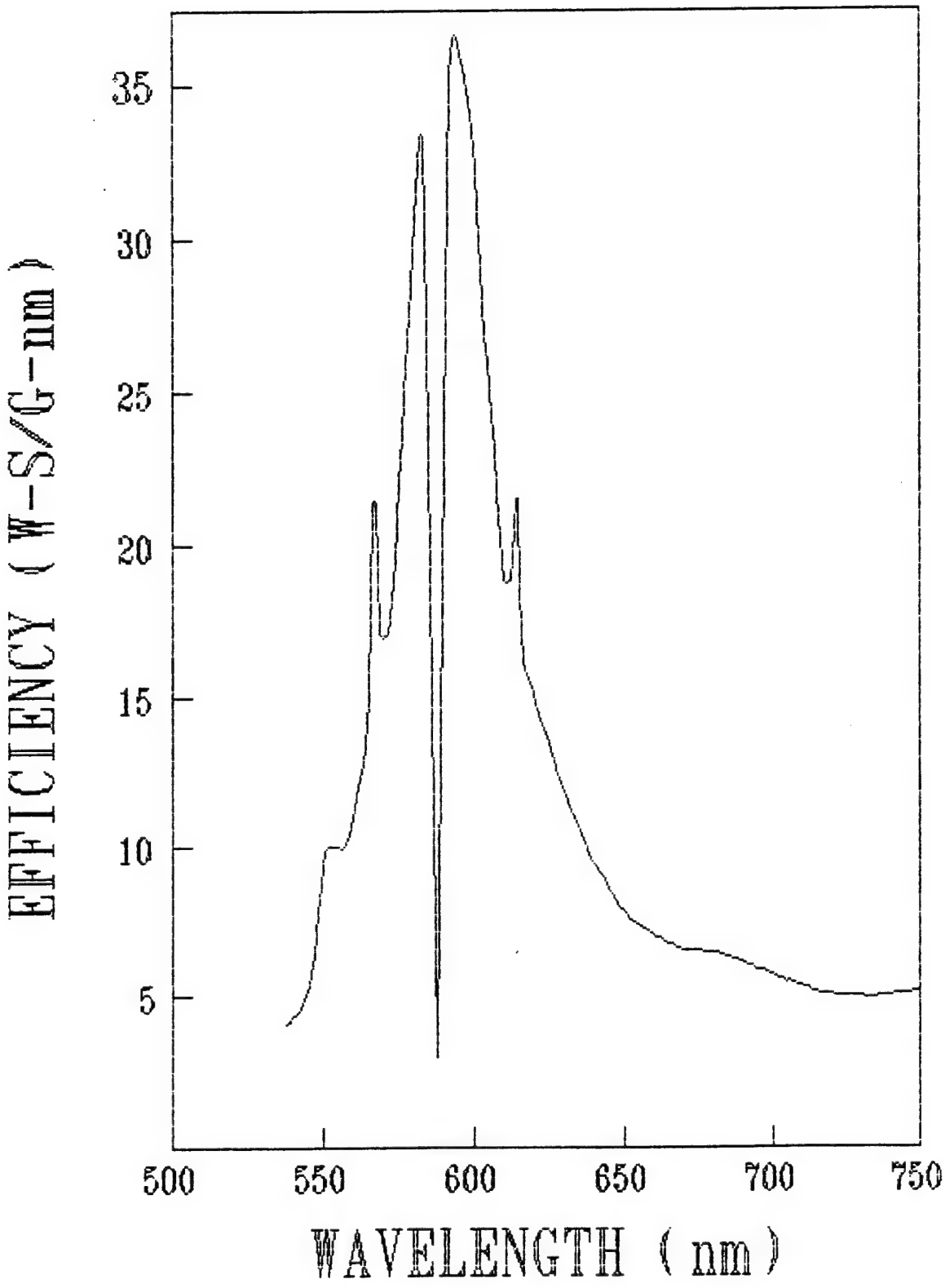

Figure 4
Spectrum of Mg-$NaNO_3$ composition showing broadened Na emission line

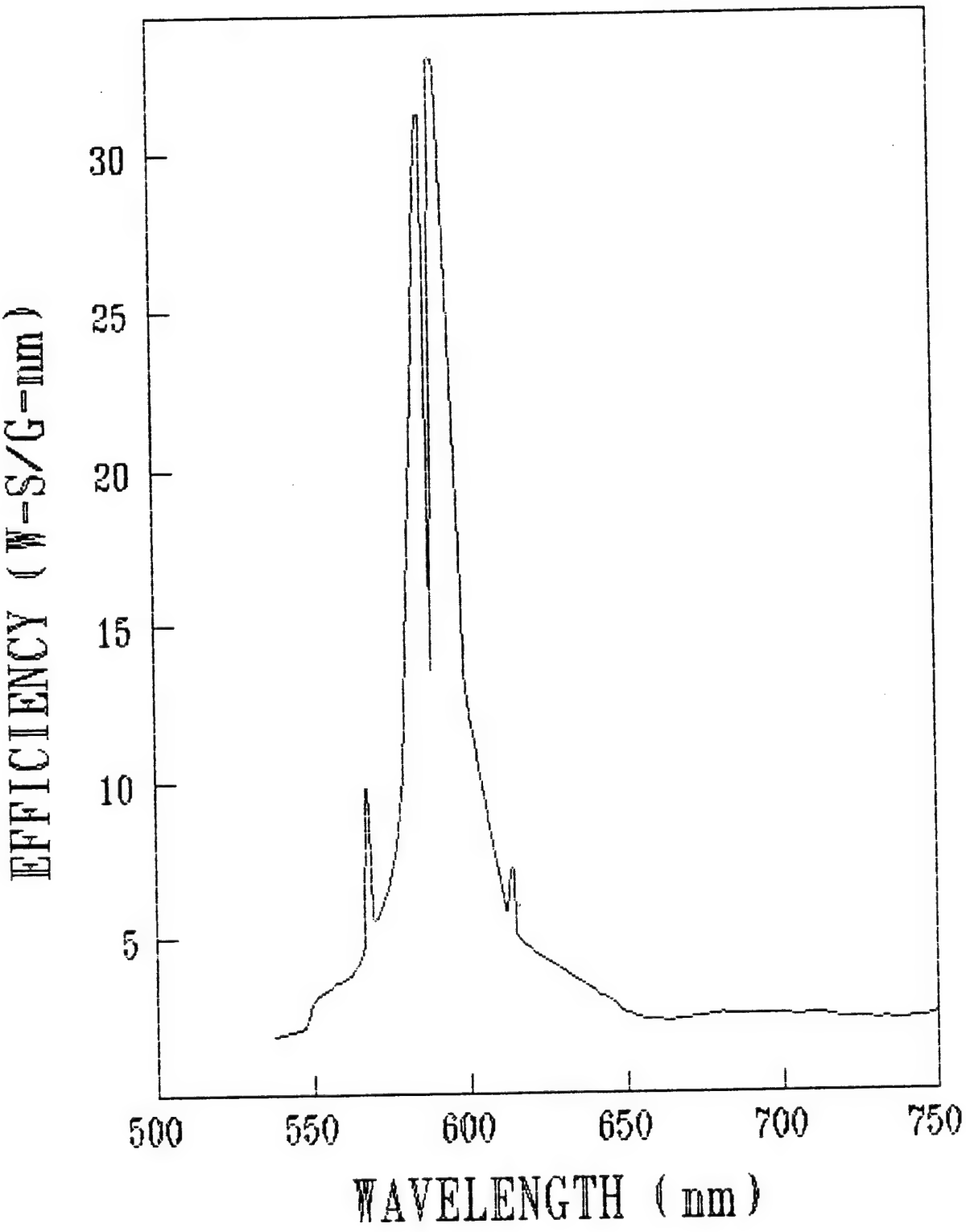

Figure 5
Spectrum of Mg-$NaClO_3$ composition

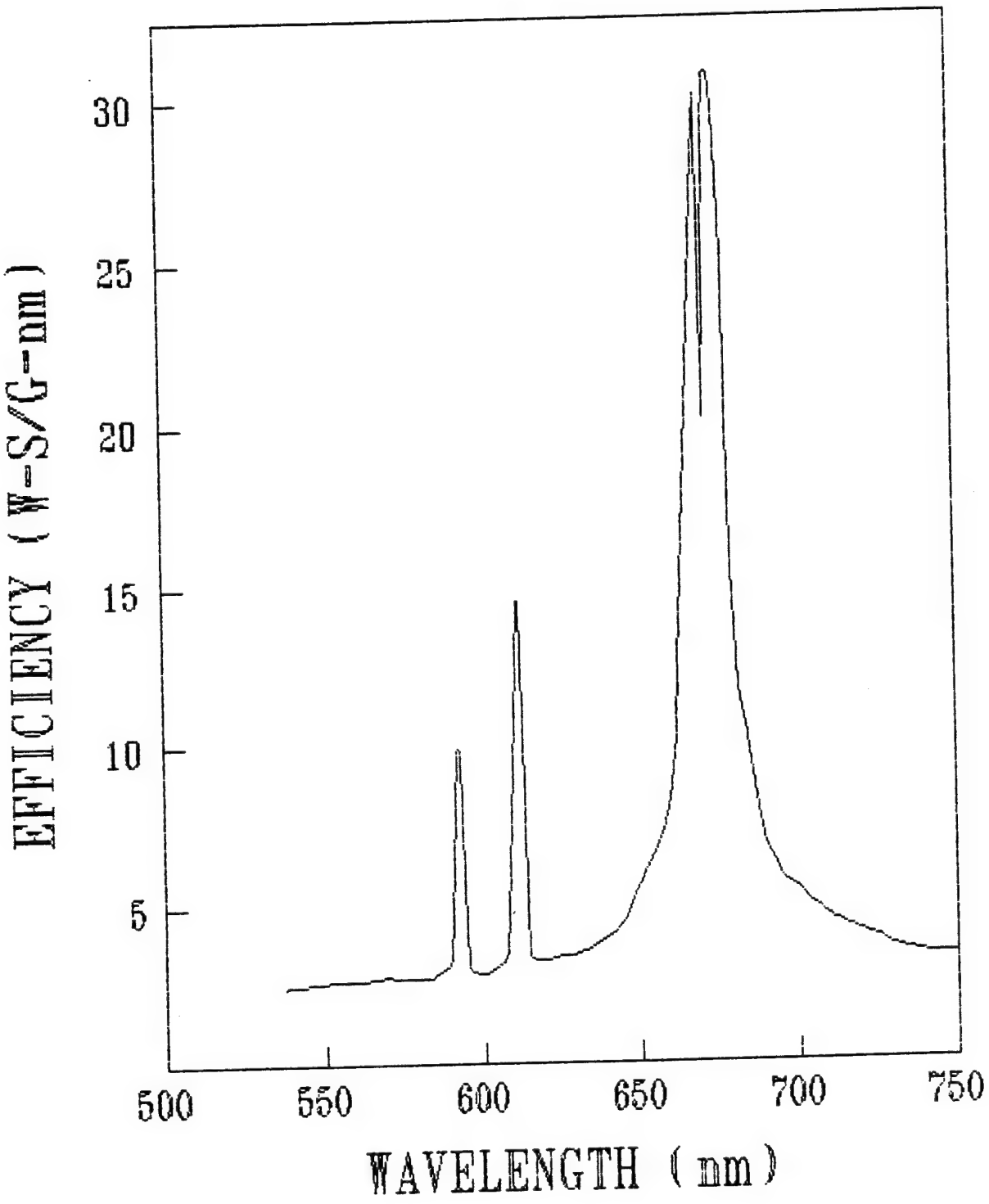

Figure 6
Spectrum of Mg-Li NO_3 composition showing broadened Li emission line

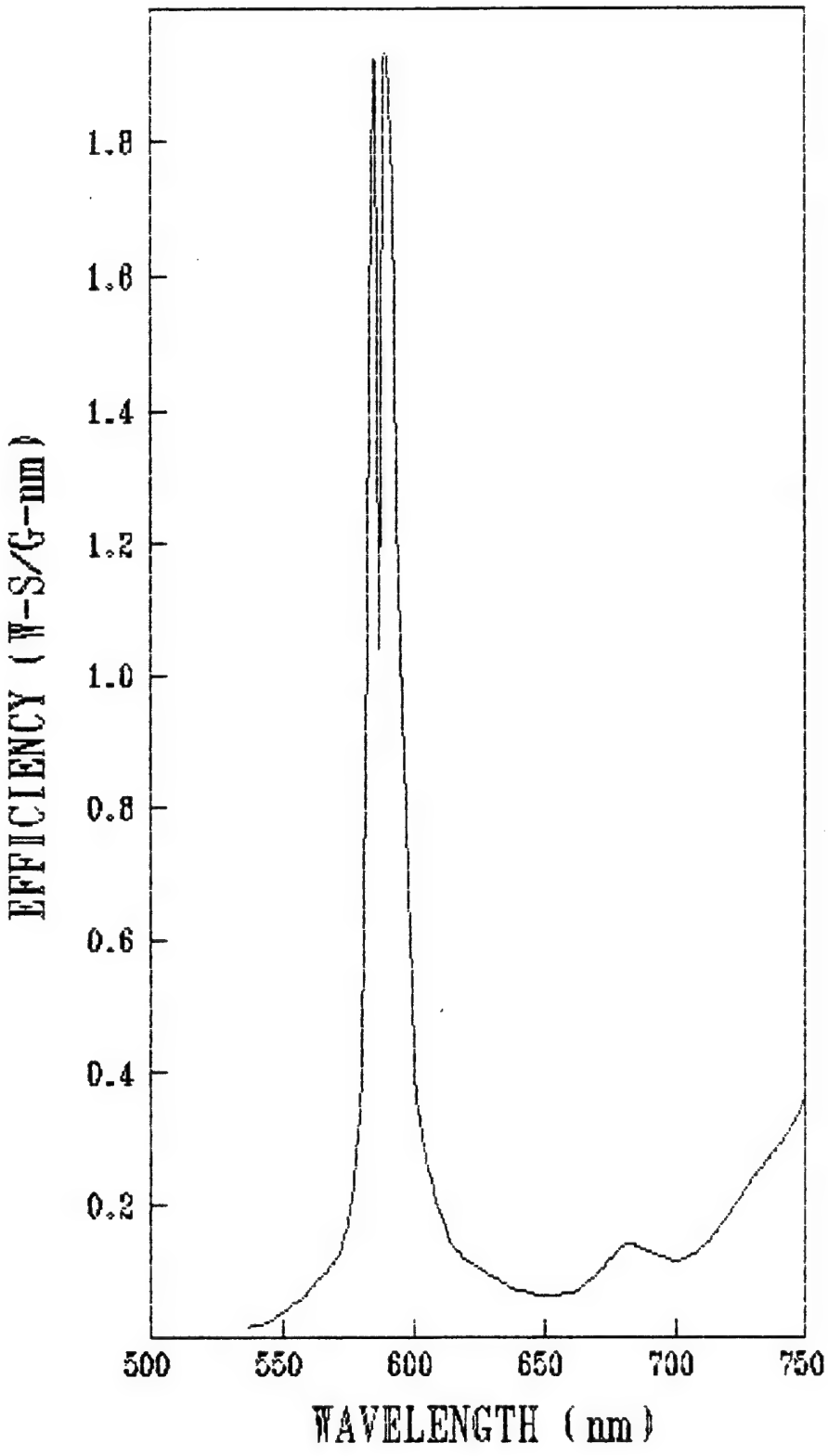

Figure 7
Spectrum of C-$NaNO_3$ composition

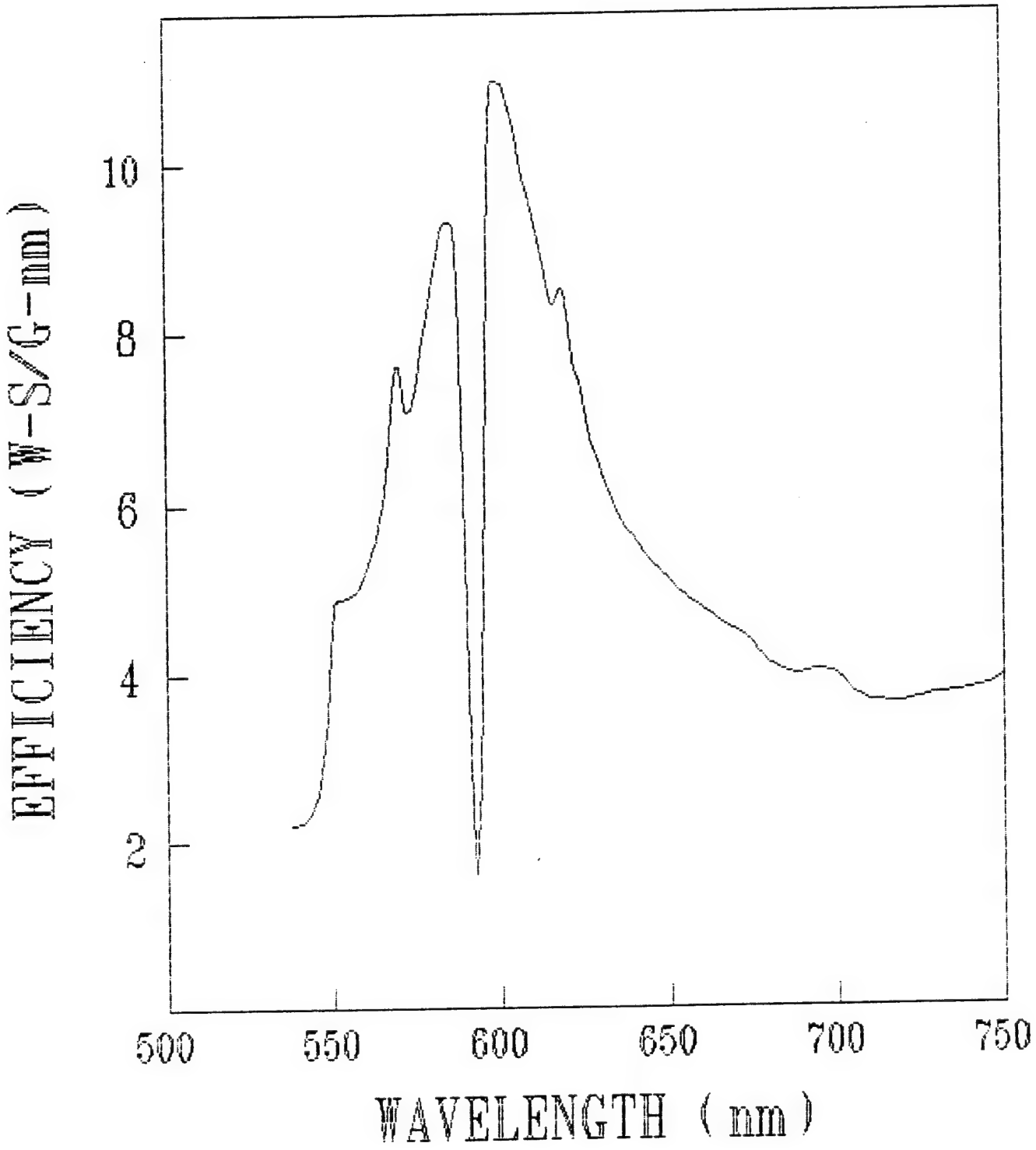

Figure 8
Spectrum of Al - $NaNO_3$ composition

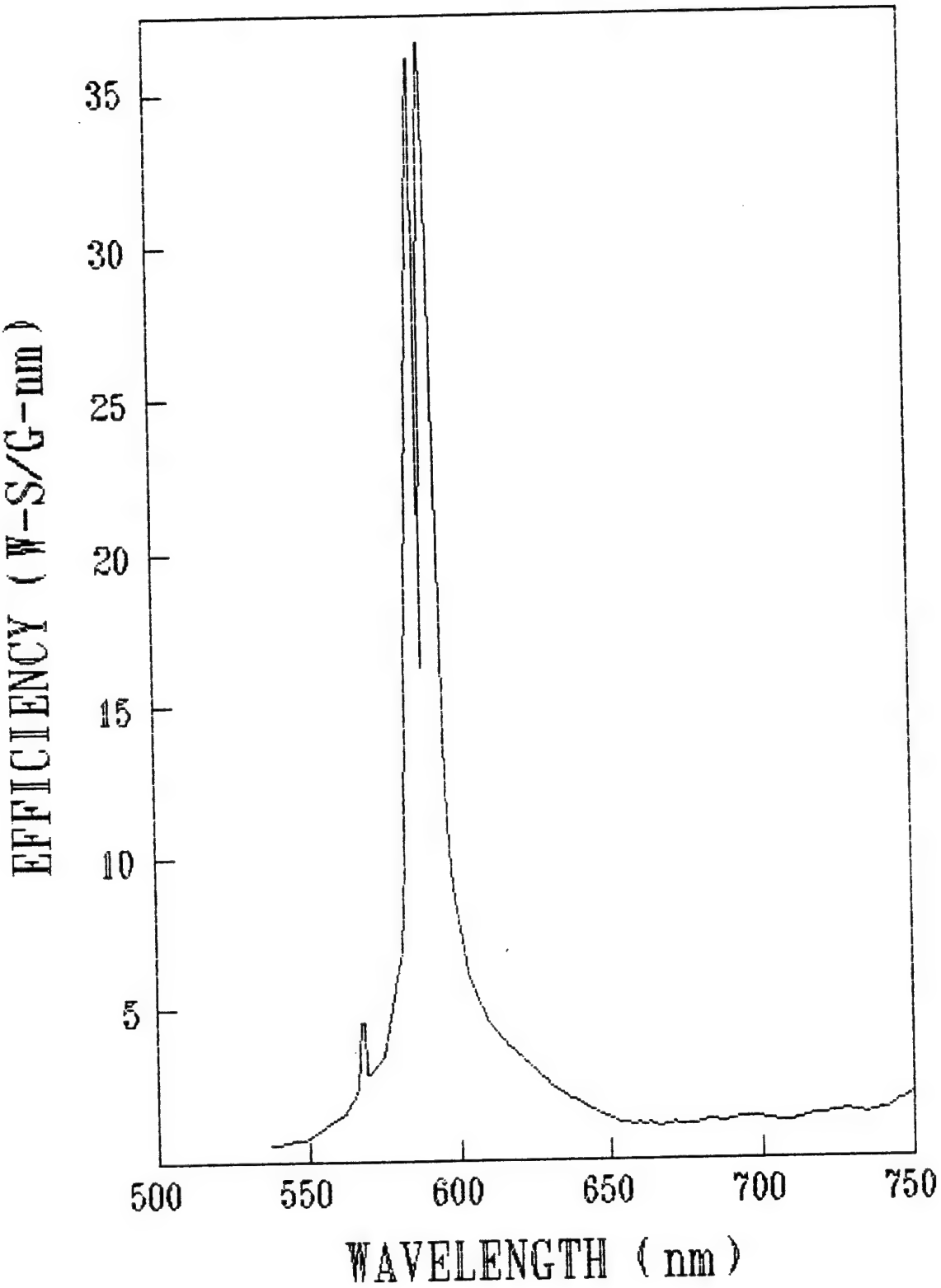

Figure 9
Spectrum of a cast Mg-$NaNO_3$ composition

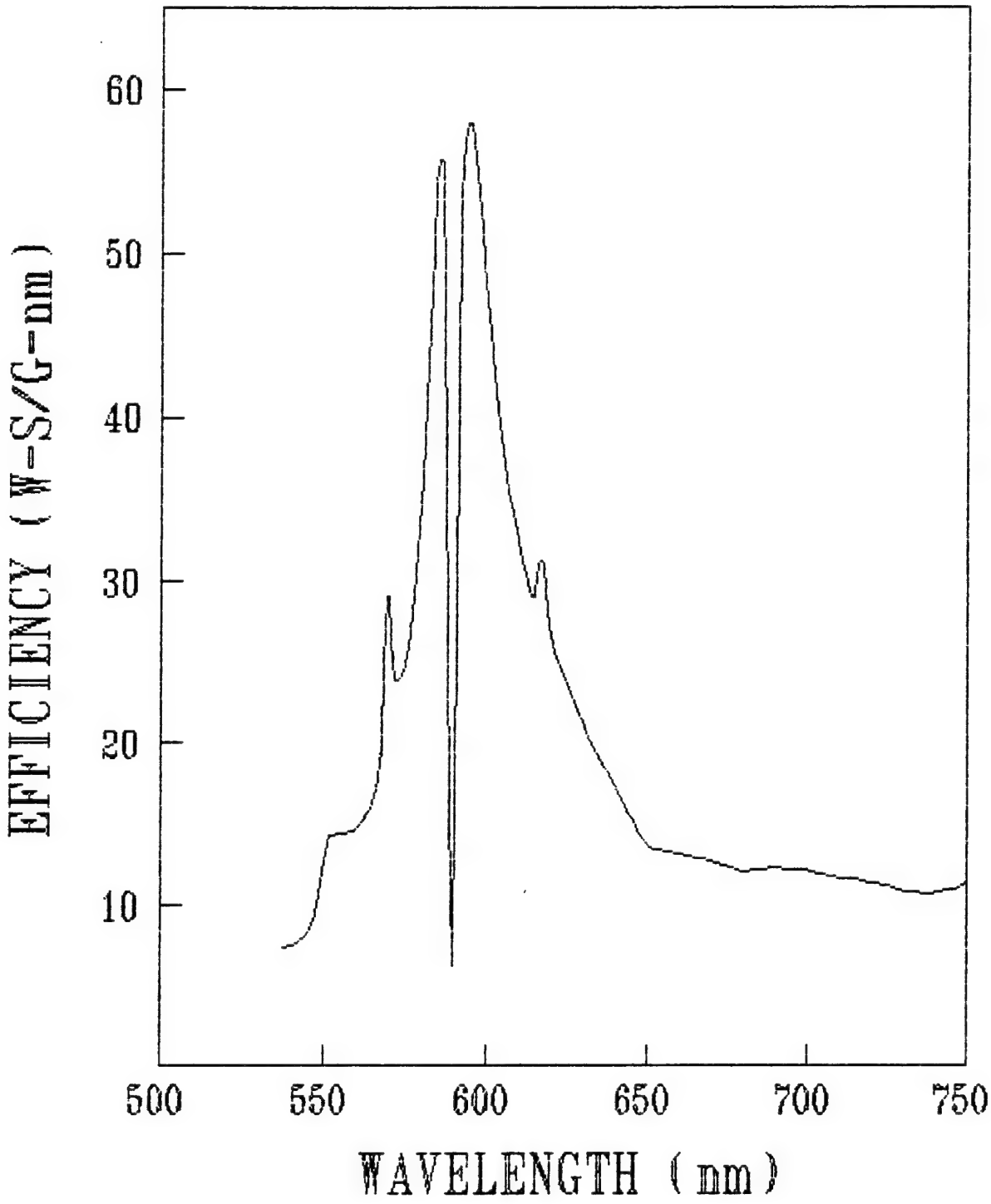

Figure 10
Spectrum of a cast Mg-$NaNO_3$ composition containing TEDGN

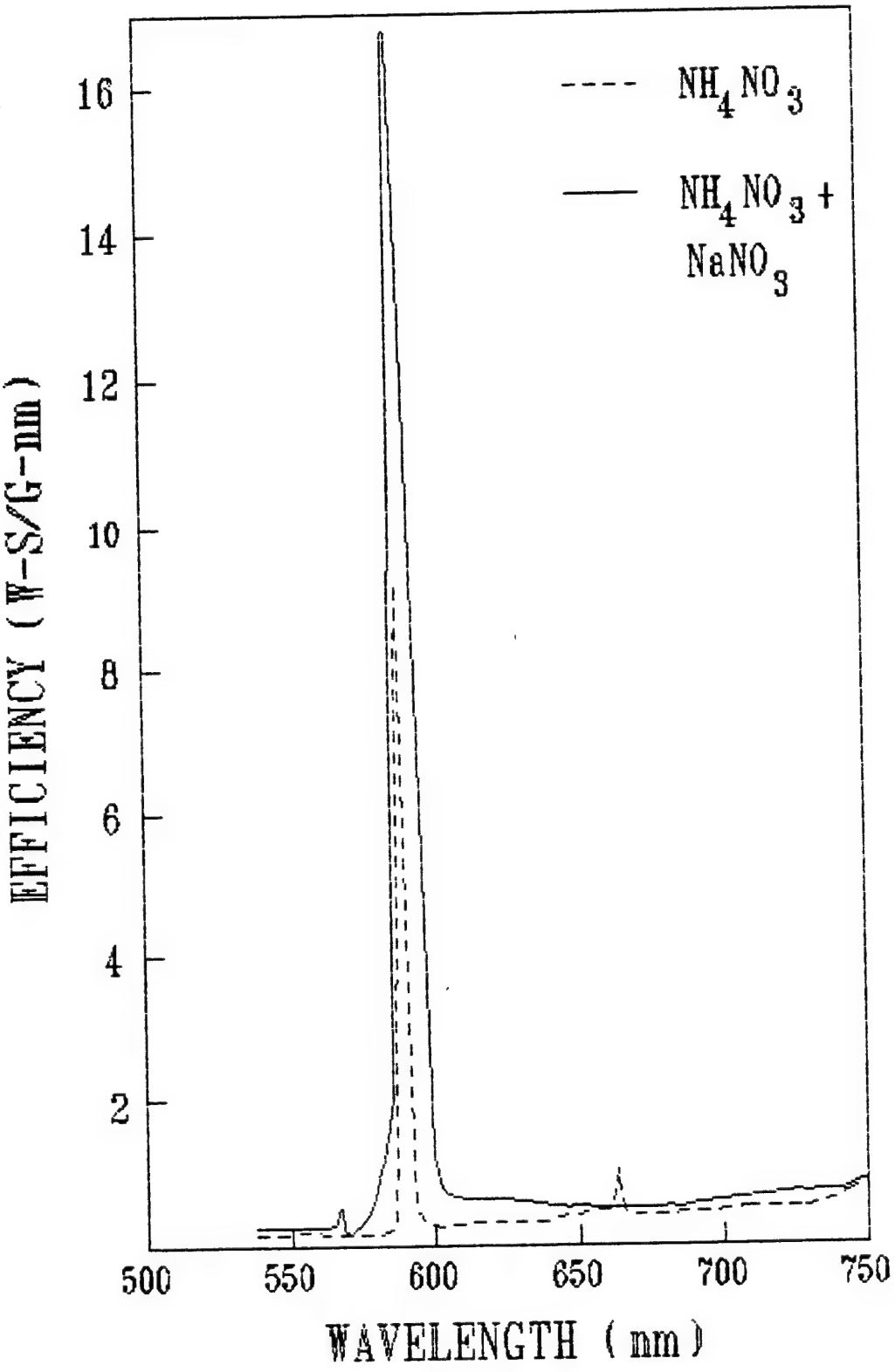

Figure 11
Spectra showing the beginning of line broadening

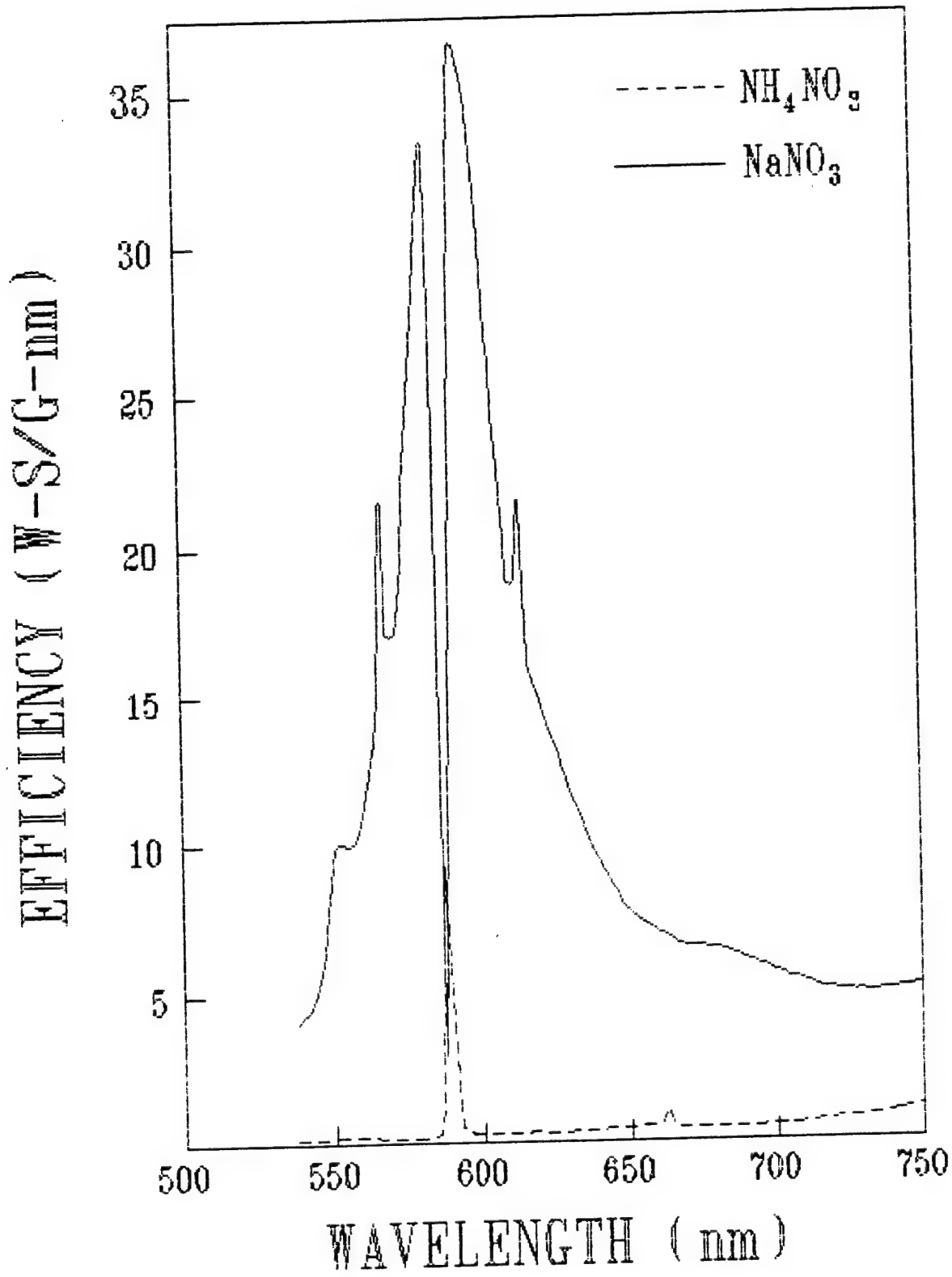

Figure 12
Specta comparing fully broadened Na line emission with an impurity Na line

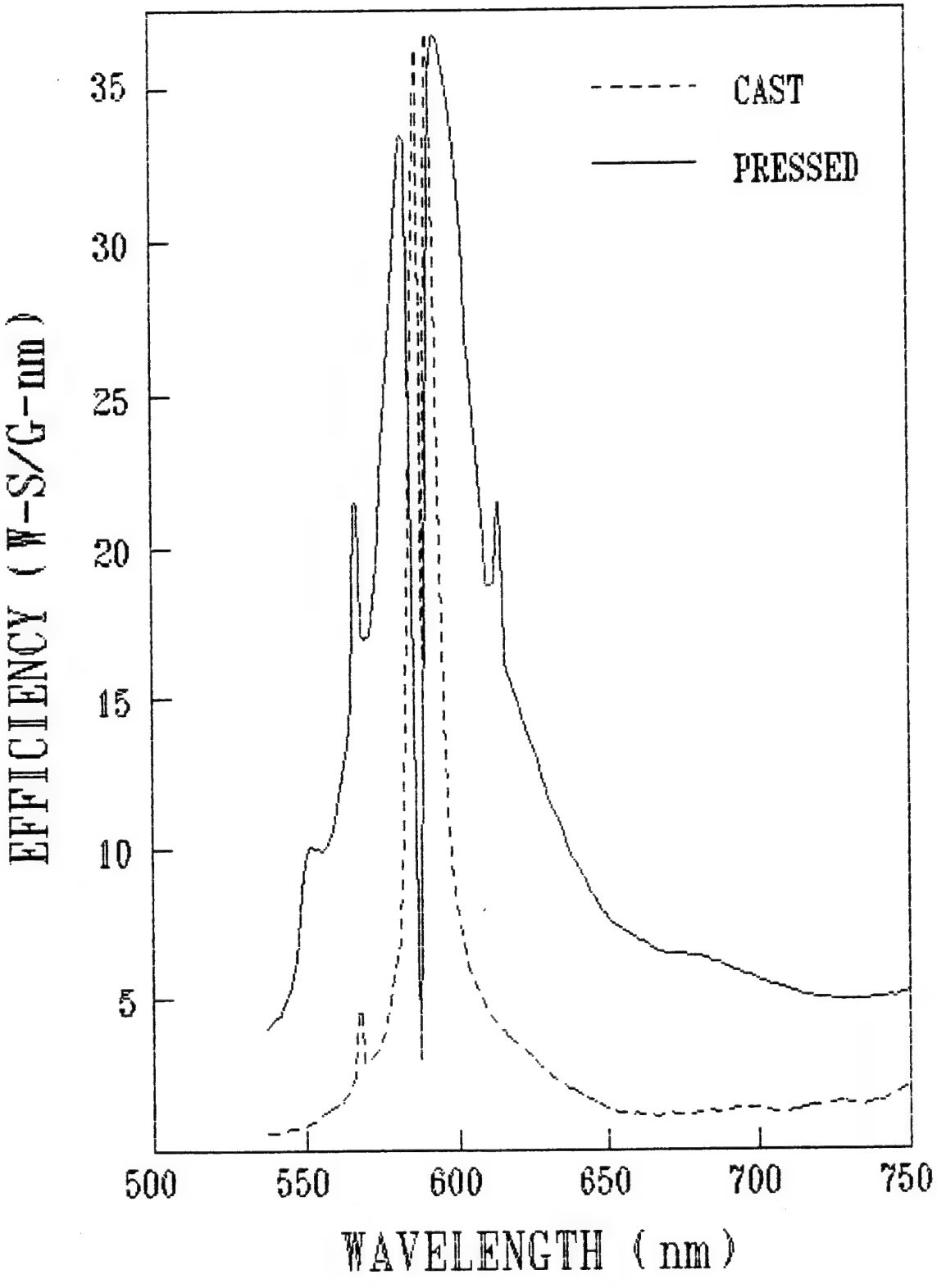

Figure 13
Spectra showing effect of casting on Na line from Mg-$NaNO_3$ composition

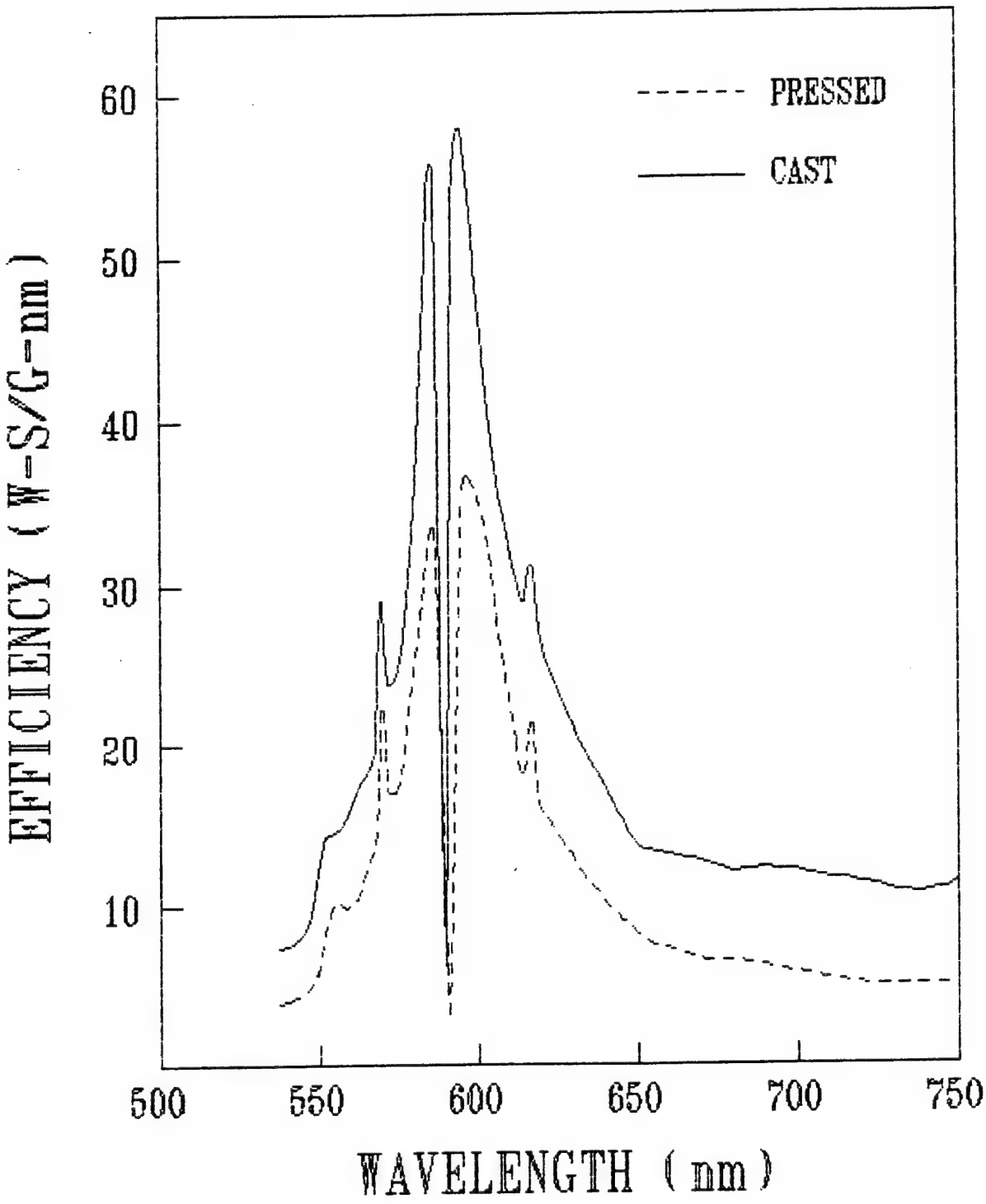

Figure 14
Spectra comparing a pressed Mg-$NaNO_3$ compositon with a cast composition containing TEGDN

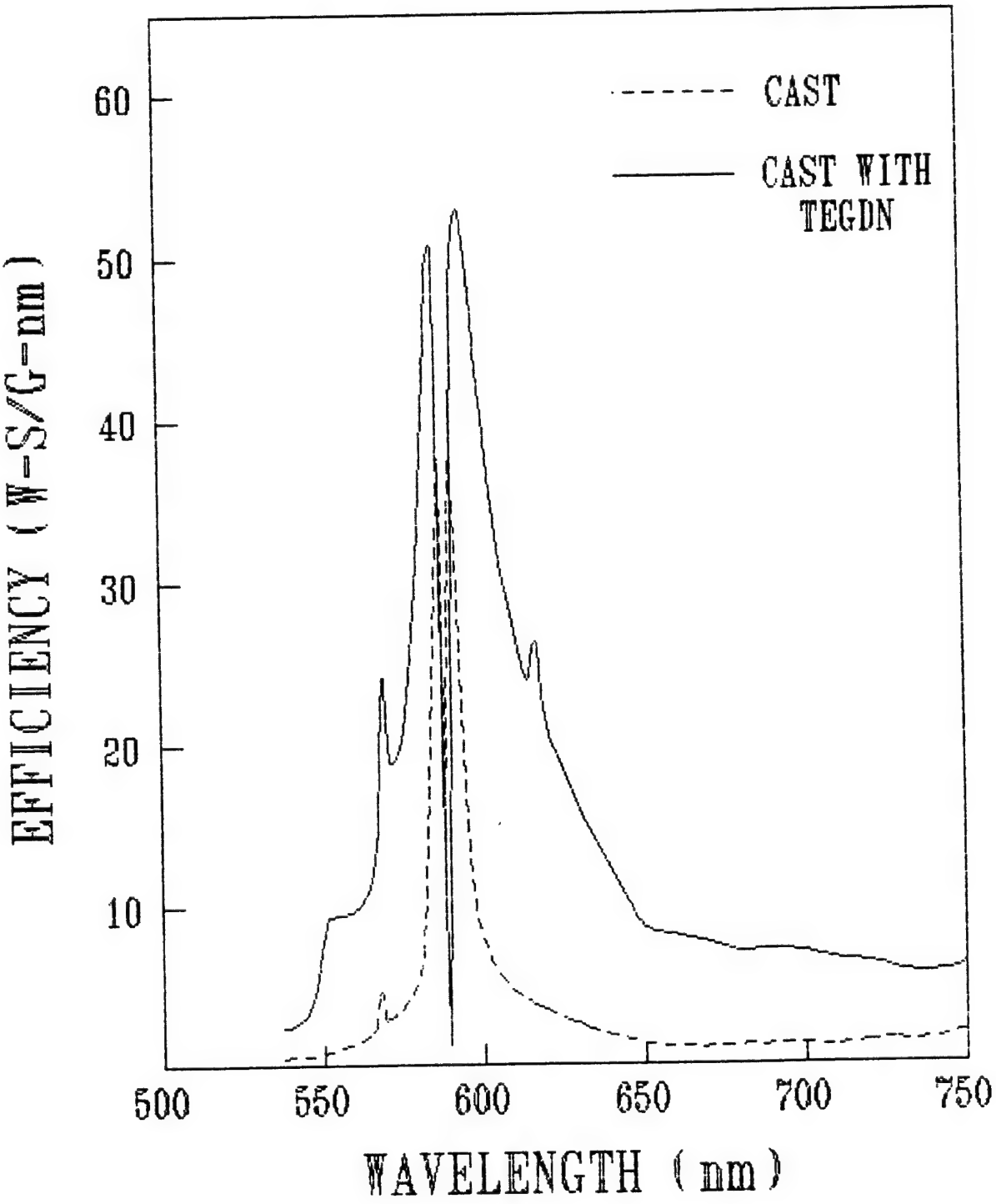

Figure 15
Spectra of cast composition showing effect of TEDGN

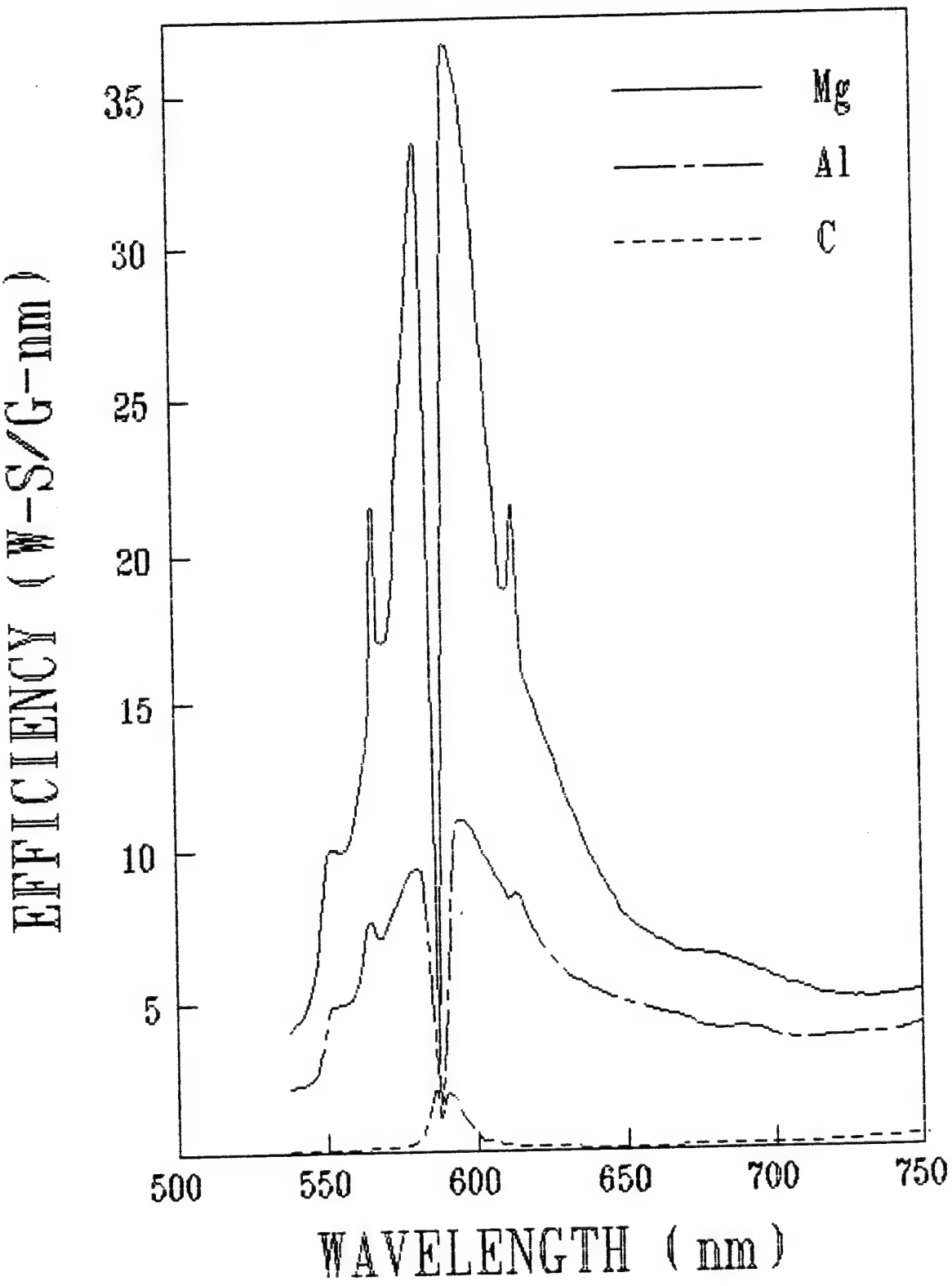

Figure 16
Spectra comparing different fuels for Mg-$NaNO_3$ compositions

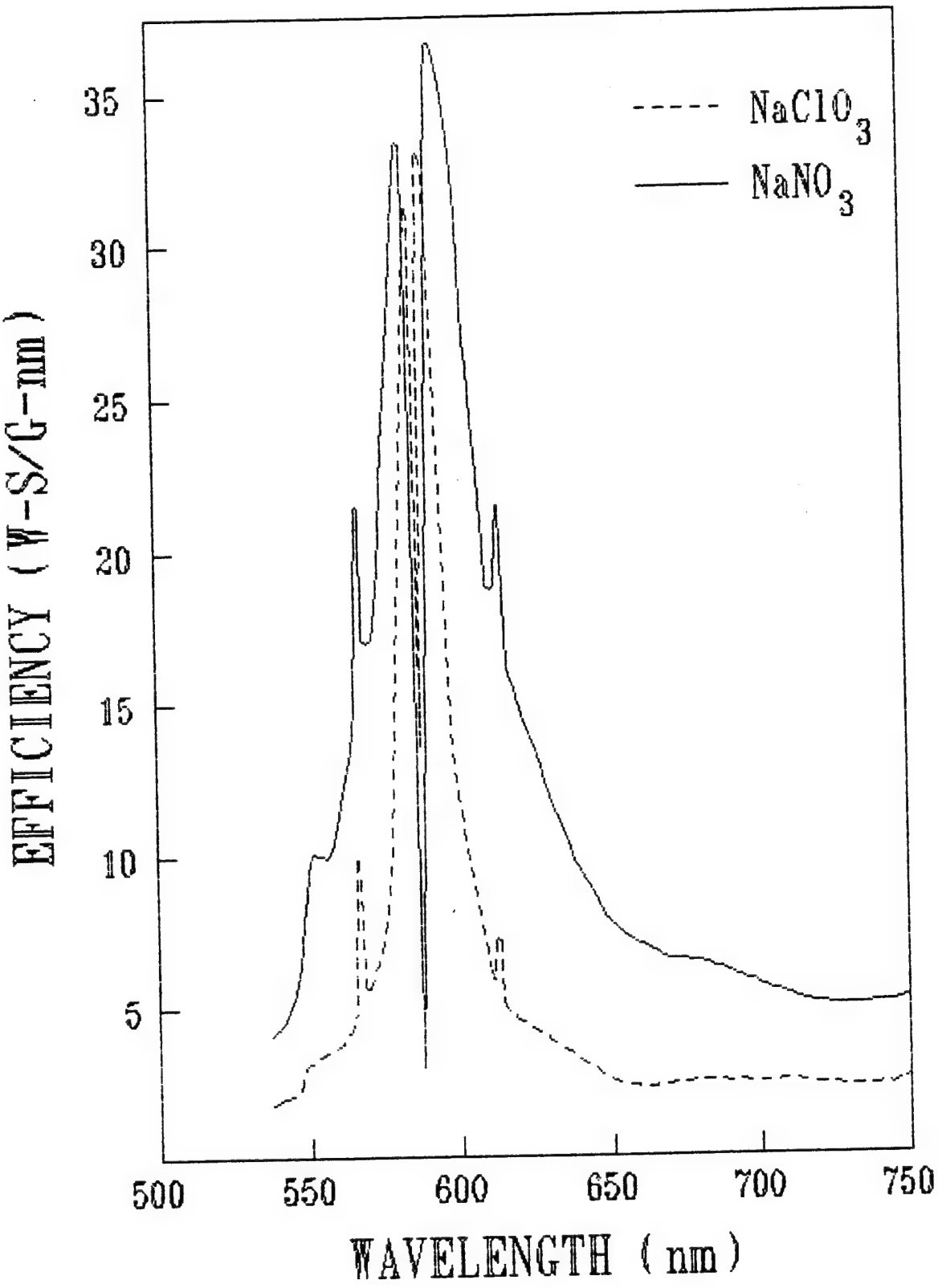

Figure 17
Spectra comparing NO_3 and $C10_3$ in the oxidant

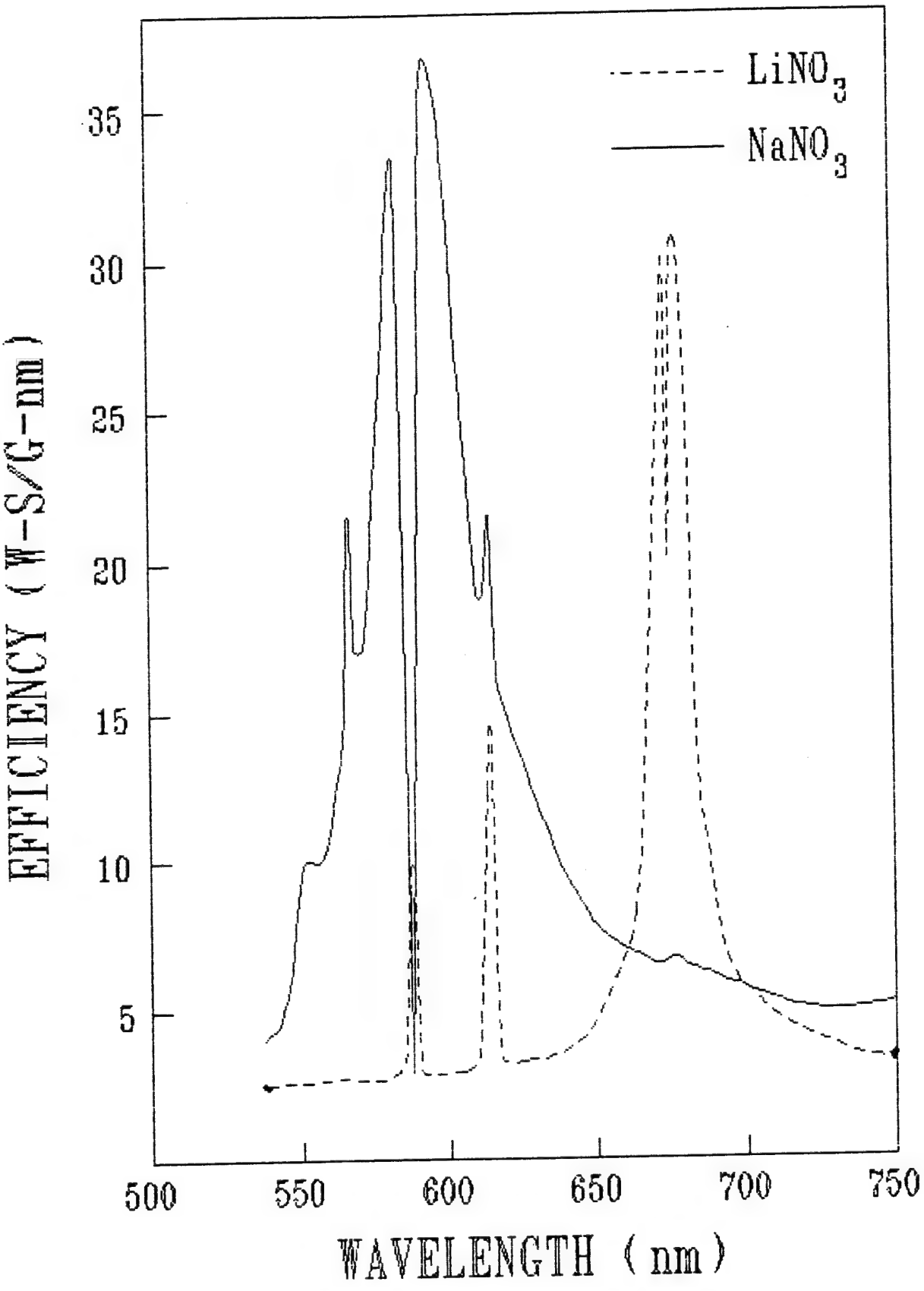

Figure 18
Spectra showing effect of using Li rather than Na in the oxidant

Table 1
Temperature and emissivity of flames

No.	Temp (k)	Peak emissivity	Greybody emissivity	Percent peak/total energy
1511	3050	0.29	0.008	18
1512	3060	0.53	0.008	51
1513	3410	0.25	0.037	59
1514	3350	0.39	0.025	51
1515	3460	0.22	0.023	52
1516	2250	0.92	0.026	59
1517	2850	*	---	56
1518	2960	0.61	0.022	49
1519	2900	0.80	0.079	59

(*) Plume area unkown, thus black body energy could not be calculated.

Table 2
Spectral data from spectroscopic curves

No.	Spectral energy (W)	specfic energy (W/cm fl. area)	Percent BB 450 to750	Black body energy (W)	Percent spectra/BB energy
1511	43	0.56	11.1	4340	1.0
1512	70	0.97	11.3	4310	1.6
1513	2513	8.00	15.7	38070	6.6
1514	1418	5.44	14.8	27640	5.1
1515	2413	6.36	16.3	50610	4.8
1516	20	0.35	2.7	320	6.3
1517	711	*	8.6	---	---
1518	606	1.85	9.8	14070	4.3
1519	10670	7.30	9.3	54900	19.4

* Flame Area Unknown

Table 3
Thermodynamic Data

No.	ΔH_R[a] (W)	ΔH[b] (W)[h]	Available energy	Spectral energy	Percent spectral/ avail. E	Percent specific/BB E
1511	7790	3080	4710	43	0.9	1.0
1512	8000	3180	4820	70	1.5	1.6
1513	13900	6730	7170	2513	35.0	6.6
1514	18300	7220	11080	1418	13.0	5.1
1515	22200	11600	10600	2413	23.0	4.8
1516	6600	1710	4890	20	0.4	6.3
1517	16740	9740	7000	711	11.0	- -
1518	21400	8360	13040	606	4.7	4.3
1519	9800	27700	42100	10670	25.0	19.4

a H_R = energy from the reaction.
b H_{hR} = energy used to heat reagents.

Table 4
Emission energy from sodium atoms

No.	Calculated energy from one emission per Na atom	Energy in Na peak	Percent calculated/peak energy
1511	impurity only	8	-
1512	42	36	116
1513	1656	1438	112
1514	1552	723	14
1515	3057	1255	244
1516	1794	12	15120
1517	1364	398	392
1518	1227	297	449
1519	4456	6295	71

Table 5
List of Compositions

No.	Composition
1511	47.5% Mg (30/50) - 47.5% NH_4NO_3 . 5% Laminac
1512	47.5% Mg (30/50) - 45.1% NH_4NO_3 . 2.4% $NANO_3$-5% Laminac
1513	47.5% Mg (30/50) - 47.5% Na NO_3 - 5% Laminac
1514	47.5% Mg (30/50) - 47.5% Na ClO_3 - 5% Laminac
1515	47.5% Mg (30/50) - 47.5% Li NO_3 - 5% Laminac
1516	29% C - 68% $NANO_3$ - 3% Laminac
1517	47.5% A1 - 47.5% $NANO_3$ - 5% Laminac
1518	25% Mg (30/50) - 25% (50/100) - 30% $NANO_3$ - 20% Laminac
1519	25% Mg (30/50) - 25% (50/100) - 30% $NANO_3$ - 10% TEDGN - 10% Laminac

Table 6
Output data from burning pyrotechnic compositions

No.	Bt (s)	Br (cm/s)	Lo (c/cm^2)	Le (c-s/gm)
1511	70	0.086	160	1170
1512	68	0.083	330	2430
1513	34	0.208	14070	48300
1514	29	0.204	8310	23600
1515	20	0.317	5320	10800
1516	45	0.141	100	450
1517	36	0.148	4670	17000
1518	40	0.134	1980	8830
1519	12	0.436	26350	36000

Table 7
Sodium peak position and peak width

No.	Peak wave length (nm)	Peak height (w)	Peak width at half height (nm)
1511*	588	4.0	3.6
1512*	587	7.2	4.4
1513	596	33.1	38.0
1514	592	36.3	17.2
1515	672	47.2	15.6
1516	590	0.8	13.2
1517	590	9.2	80.2
1518	590	27.5	11.2
1519	592	138.0	34.4

* All peaks except for numbers 1511 and 1512 are strongly reversed.

REFERENCES

1. Ellern, R., Military and Civilian Pyrotechnics, Chemical, New York, 1968.

2. Douda, B.E., Blunt, R.M., and Bair, E.J., Journal of the Optical Society of America, 60, 1166 (1970).

3. Dinerman, C.E., "An Attempt to Increase the Luminous Output of Magnesium-Sodium Nitrate Flares by the Introduction of Nitrogen-Containing Flares," RDTR No. 278, Naval Ammunition Depot, Crane, IN, June 1974.

4. Taylor, F.R., Farnell, P.L., and Westerdahl, R.P., US Patent 3,664,898 (1972).

5. Douda, B.E. and Bair, E.J., Journal of the Optical Society of America, 60, 1257 (1970).

6. Douda, B.E., "Radiative Transfer Model of a Pyrotechnic Flame," RDTR No. 258, Naval Ammunition Depot, Crane, IN, September 1973.

7. Beardell, A.J., Farnell, P.L., Anderson, D.A., and Taylor, F.R., Analysis of the Potential for the Improvement of Illuminating Flare Performance,' WAG-2 Battlefield Illumination Seminar, Dover, NJ, August 1973.

8. Westerdahl, R.P., unpublished work, 1979.

APPENDIX

Equations Used to Calculate Tabular Data

(1) Planck equation: Black body intensity at a specific λ and T

$$I_{BB} = c_1/\lambda^5 (e^{c2/\lambda T}-1)^{-1}$$

where

C_1 and C_2 are constants

λ^1= wavelength in cm

T = temperature in °K

(2) Peak $\varepsilon = I_{pk} \times 10^7 / I_{BB}$ x flame area

where

Peak ε = emissivity of the spectral peak

I_{pk} = energy of peak in w/nm

flame area is in cm^2

10^7 = conversion factor from nm to cm

(3) Grey body emissivity = I_{GB} /$_{BB}$ at 475 nm

Intensities are at 475 nm (no spectral emission)

(4) $E_{BB} = \sigma T^4$ x flame area x % $BB_{450-750}$

where

E_{BB} = calculated black body energy between 450 and 750 nm

σ = Stefan- Boltzmann constant

T = temperature in °K

flame area in cm^2

% $BB_{4450-750}$ = % of BB energy between 450 and750 nm

(σT energy is for zero to infinity wavelength)

(5) % of spectral energy in peak = $100 (E_{tot} - (\varepsilon_{GB} \times E_{BB}) / E_{tot}$

where

E_{tot} = Integrated energy measured from spectrum of flare

ε_{GB} = emissivity of the grey body background from Eq (3)

E_{BB} = from Eq (4)

(6) $\Delta H_{f\text{-}ox} = \Delta H_{R1} \times \frac{\text{wt. ox x \% fuel}}{\text{\% ox}}$

where

$\Delta H_{f\text{-}ox}$ = calculated heat for the fuel-oxidant reaction

ΔH_{R1} calculated heat per gram of fuel for the reaction

percentages are for the stoichiometric reaction weights are total amount of constituent in composition (latter two used to calculate amount of fuel that will react with amount of oxidant present)

(7) $\Delta H_{f\text{-}air} = \Delta_{R2} \times (\text{wt. fuel} - \frac{\text{wt. ox x \% fuel}}{\text{\% ox}})$

where

$\Delta H_{f\text{-}air}$ = calculated heat of excess fuel with air reaction

ΔH_{R2} calculated heat per gram of fuel for reaction the rest calculates the amount of excess fuel available

(8) $\Delta H_R = \Delta H_{f\text{-}ox} + \Delta H_{f\text{-}air}$

where

ΔH_R= calculated total heat for the composition

$\Delta H_{f\text{-}ox}$ and $\Delta H_{f\text{-}air}$ are from Eqs (6) and (7)

(9) $\Delta H_h = \Delta H_{\text{to MP}} + \Delta H_{fusion} + \Delta H_{\text{to BP}} + \Delta_{vap} + \Delta H_{\text{to flame temp}}$

where

ΔH_h = energy needed to heat ingredients to flame temp

$\Delta H_{\text{to MP}}$ = energy to heat to melting points (MP)

ΔH_{fusion}= energy to melt

$\Delta H_{\text{to BP}}$ = energy to heat from MP to boiling points (BP)

ΔH_{vap} = energy to vaporize

$\Delta H_{\text{to flame temp}}$ = energy to heat from BP to flame temp

(10) % of available E = $100 \times E_{tot} / (\Delta H_R - \Delta H_h)$

where

E_{tot} = spectral energy measured for flare (see Eq (5))

ΔH_R and ΔH_h are from Eqs (8) and (9)

(11) $E_{Na} = hc/\lambda$

where

E_{Na} = the energy from one Na atom emission in w-s

h = Planck's constant

c = velocity of light

λ = wavelength of emission

(12) $E_{em} = (E_{Na} \times N_o \times moles_{Na}) / BT$

where

E_{em} = total energy from one emission per Na atom in flare

E_{Na} from Eq (11)

N_o = Avagadro's number

$moles_{Na}$ = moles of Na (or Li) in composition

BT = burning time in seconds

DISTRIBUTION LIST

Commander
Armament Research, Development and Engineering Center
U.S. Army Armament, Munitions and Chemical Command
ATTN: AMSTA-AR-IMC (3)
AMSTA-AR-GCL (D)
AMSTA-AR-AEE, Joseph Lannon (3)
AMSTA-AR-AEE-P, Russell Broad (5)
Picatinny Arsenal, NJ 07806-5000

Administrator
Defense Technical Information Center
ATTN: Accessions Division (12)
Cameron Station
Alexandria, VA 22304-6145

Director
U.S. Army Material Systems Analysis Activity
ATTN: AMXSY-MP
Aberdeen Proving Ground, MD 21005-5066

Commander
Chemical/Biological Defense Agency
U.S. Army Armament, Munitions and Chemical Command
ATTN: AMSCB-CII, Library
SMCCR-MU
SMCCR-MUS-A
Aberdeen Proving Ground, MD 21010-5423

Director
U.S. Army Edgewood Research, Development and Engineering Center
ATTN: SCBRD-RTT (Aerodynamics Technical Team)
Aberdeen Proving Ground, MD 21010-5423

Director
U.S. Army Research Laboratory
ATTN: AMSRL-OP-CI-B, Technical Library
Aberdeen Proving Ground, MD 21005-5066

Chief
Benet Weapons Laboratory, CCAC
Armament Research, Development and Engineering Center
U.S. Army Armament, Munitions and Chemical Command
ATTN: SMCAR-CCB-TL
Watervliet, NY 12189-5000

Director
U.S. Army TRADOC Analysis Activity
ATTN: ATAA-SL
White Sands Missile Range, NM 88002

Director
Ballistic Research Laboratory
ATTN: AMXBR-OD-ST
Aberdeen Proving Grounds, MD 21005-5066

U.S. Army Foreign Science and Technology Center
220 Seventh Street, NE
Charlottesville, VA 22901-5396

U.S. Army Research Office
ATTN: RDRD
P.O. Box 12211
Research Triangle Park, NC 27709

Commander
Naval Weapons Support Center
ATTN: Code 502
Crane, IN 47522-5050

Commander
Naval Weapons Center
ATTN: Code 3880
Code 233, Technical Library
China Lake, CA 93555-6001

Commander
Naval Surface Weapons Center
White Oak Laboratory
ATTN: Code X-21, Tech Library
Silver Springs , MD 20910

Commander
Naval Air Systems Command
ATTN: Code AIR-954, Technical Library
Washington, DC 20361

Commander
Naval Sea Systems Command
ATTN: SEA-09G3, Technical Library
Washington, DC 20362-5101

Commander
U.S. Naval Ordnance Station
ATTN: Code 5124
Scientific and Tech Info Div
Indian Head, MD 20640-5000 .

Commander
U.S. Air Force
ATTN: Library
Eglin Air Force Base, FL 32542

Aeronautical Systems Division
ATTN: WRDC/ISL, Technical Library
Wright-Patterson Air Force Base, OH, 45433-6503

Commander
Air Force Wright Research and Development Center
ATTN: WRDC/AAWW-3
WRDC/AAWA-I/EW TIC
Wright-Patterson Air Force Base, OH, 45433-6543

Commander
Harry Diamond Laboratories
ATTN: Library, Room 211, Bldg 92
Connecticut Ave. and Van Ness Street, NW
Washington, DC 20438

Defense Intelligence Agency
ATTN: DT-3B
Washington, DC 20301

Institute for Defense Analyses
ATTN: Library, Documents
1801 Beauregard Street
Alexandria, VA 22311